A novel family of heteroleptic 1D chain spin-crossover complexes and its DFT modelling. How the formation of polynuclear chains modifies the ligand-field effects on spin transition

Vladyslav Maliuzhenko,[a] Marek Weselski,[a] Maria Książek,[b] Tim Hochdörffer,[c] Juliusz A. Wolny,*[c] Volker Schünemann,[c] Joachim Kusz,[b] Robert Bronisz*[a]

[a] Msc V. Maliuzhenko, Dr M. Weselski, Dr R. Bronisz
Faculty of Chemistry,
University of Wrocław,
F. Joliot-Curie 14, 50-383, Wrocław, Poland
E-mail: robert.bronisz@uwr.edu.pl

[b] Dr M. Książek, Prof. J. Kusz,
Institute of Physics,
University of Silesia,
75 Pułku Piechoty 1, 41-500 Chorzów, Poland

[c] Dr T. Hochdörffer, Dr. J. A. Wolny, Prof. V. Schünemann,
Department of Physics,
RPTU Kaiserslautern-Landau,
Erwin Schrödinger Str. 46 67663 Kaiserlautern, Germany

Table S1. Crystallographic data for crystal structures of **1**, **2**, **3** and **4**.

CCDC No.	**2259411**	**2259412**	**2259413**	**2259414**	**2259415**	**2259416**	**2259417**	**2259418**
Compound	**1**		**2**		**3**		**4**	
Temperature	**100 K**	**480 K**	**100 K**	**480 K**	**80 K**	**250 K**	**90 K**	**250 K**
Spin state	**LS**	**HS**	**LS**	**HS**	**LS**	**HS**	**HS**	**HS**
Empirical formula	$C_{20}H_{22}B_2F_8FeN_{18}$	$C_{20}H_{22}B_2F_8FeN_{18}$	$C_{20}H_{22}B_2F_8FeN_{18}$	$C_{20}H_{22}B_2F_8FeN_{18}$	$C_{24}H_{27}B_2F_8FeN_{17}$	$C_{24}H_{27}B_2F_8FeN_{17}$	$C_{23}H_{28}B_2F_8FeN_{16}O$	$C_{23}H_{28}B_2F_8FeN_{16}O$
Formula weight	744.02	744.02	744.02	744.02	783.09	783.09	773.83	773.83
Crystal system	triclinic	triclinic	triclinic	triclinic	triclinic	triclinic	monoclinic	monoclinic
Space group	*P-1*	*P-1*	*P-1*	*P-1*	*P-1*	*P-1*	*C2/c*	*C2/c*
a/Å	7.9524(3)	8.2850(18)	8.5402(4)	8.872(2)	12.1787(8)	12.4510(8)	15.7477(8)	15.7542(7)
b/Å	8.8207(2)	9.0556(10)	8.8402(3)	8.946(2)	12.5849(10)	12.5509(9)	12.9089(5)	12.9367(6)
c/Å	9.9917(3)	10.3075(12)	9.8635(7)	10.078(2)	13.0995(12)	13.2455(10)	15.3724(10)	15.6423(9)
α/°	86.989(2)	86.883(10)	84.319(5)	85.350(19)	115.979(8)	117.927(7)	90	90
β/°	84.475(3)	83.973(13)	78.000(5)	74.76(2)	110.675(7)	110.260(6)	100.050(6)	100.243(5)
γ/°	85.069(3)	83.689(14)	83.464(3)	85.05(2)	98.201(6)	95.241(5)	90	90
Volume/Å^3	694.35(4)	763.7(2)	721.48(7)	767.5(3)	1579.6(2)	1633.5(2)	3077.0(3)	3137.2(3)
Z	1	1	1	1	2	2	4	4
ρ_{calcg}/cm^3	1.779	1.618	1.712	1.610	1.646	1.592	1.670	1.636
μ/mm^{-1}	0.650	0.591	5.127	0.588	4.708	4.553	0.591	0.579
Radiation	MoKα	MoKα	CuKα	MoKα	CuKα	CuKα	MoKα	MoKα
2Θ range for data collection/°	6.054 to 52.732	5.898 to 52.744	9.194 to 147.054	6.386 to 52.74	8.19 to 147.11	7.95 to 147.564	6.312 to 52.744	6.298 to 52.744
Index ranges	-9 ≤ h ≤ 9 -11 ≤ k ≤ 10 -12 ≤ l ≤ 11	-10 ≤ h ≤ 10 -11 ≤ k ≤ 11 -12 ≤ l ≤ 11	-10 ≤ h ≤ 7 -10 ≤ k ≤ 10 -12 ≤ l ≤ 11	-11 ≤ h ≤ 11 -9 ≤ k ≤ 11 -12 ≤ l ≤ 12	-14 ≤ h ≤ 15 -15 ≤ k ≤ 12 -16 ≤ l ≤ 16	-14 ≤ h ≤ 15 -15 ≤ k ≤ 13 -16 ≤ l ≤ 16	-17 ≤ h ≤ 19 -16 ≤ k ≤ 16 -19 ≤ l ≤ 19	-17 ≤ h ≤ 19 -15 ≤ k ≤ 16 -19 ≤ l ≤ 19
Reflections collected	5862	6414	5085	6408	11202	11666	12632	26053
Independent reflections	2831	3132	2806	3140	6145	6347	3147	3210
R_{int}	0.0206	0.0443	0.0125	0.0407	0.0591	0.0330	0.0397	0.0709
R_{sigma}	0.0269	0.0608	0.0187	0.0552	0.1002	0.0551	0.0323	0.0403
Data/ restraints/ parameters	2831/ 18/ 233	3132/ 28/ 232	2806/ 0/ 223	3140/ 29/ 252	6145/ 0/ 489	6347/ 0/ 495	3147/ 0/ 239	3210/ 2/ 238
Goodness-of-fit on F^2	1.051	1.030	1.086	1.063	0.999	1.018	1.040	1.065
Final R indexes [I>=2σ (I)]	R_1 = 0.0343 wR_2 = 0.0847	R_1 = 0.0844 wR_2 = 0.2383	R_1 = 0.0256 wR_2 = 0.0673	R_1 = 0.0879 wR_2 = 0.2489	R_1 = 0.0606 wR_2 = 0.1377	R_1 = 0.0477 wR_2 = 0.1167	R_1 = 0.0396 wR_2 = 0.1007	R_1 = 0.0641 wR_2 = 0.1690
Final R indexes [all data]	R_1 = 0.0375 wR_2 = 0.0873	R_1 = 0.1114 wR_2 = 0.2814	R_1 = 0.0257 wR_2 = 0.0675	R_1 = 0.1328 wR_2 = 0.3102	R_1 = 0.1059 wR_2 = 0.1656	R_1 = 0.0661 wR_2 = 0.1284	R_1 = 0.0503 wR_2 = 0.1083	R_1 = 0.0855 wR_2 = 0.1936
Largest diff. peak/hole / e Å^{-3}	0.90/ -0.49	0.93/ -0.57	0.26/ -0.29	0.49/ -0.39	0.53/ -0.62	0.50/ -0.41	0.59/ -0.76	0.90/ -0.46

Table S2. Selected interatomic distances (Å), angles (°) and Σ (°) values for compounds **1** and **2**.

Compound	**1**		**2**	
Temperature	**480 K**	**100 K**	**480 K**	**100 K**
Spin state	**HS**	**LS**	**HS**	**LS**
Fe-N1(py)	2.1864(35)	2.0125(15)	2.1883(45)	2.0362(12)
Fe-N14(tz^{py})	2.1379(36)	1.9681(15)	2.1307(46)	1.9710(12)
Fe-N24(tz)	2.1972(40)	1.9763(15)	2.1407(49)	1.9729(12)
Fe-N(average)	2.1738(40)	1.1986(15)	2.1532(49)	1.1993(12)
N1(py)-Fe-N14(tz^{py})	75.27(14)	80.36(6)	76.26(17)	80.81(5)
N1(py)-Fe-N24(tz)	91.95(15)	91.36(6)	87.92(17)	88.31(5)
N14(tz^{py})-Fe-N24(tz)	89.92(15)	90.06(6)	90.51(19)	90.47(5)
N1(py)-C2-C15-N14(tz^{py})	9.611(17)	6.987(3)	2.324(40)	0.985(5)
Fe1-Fe1[a]	10.3075(12)	9.9917(3)	10.078(2)	9.8635(7)
Fe1-Fe1[b]	8.2850(18)	7.9524(3)	8.8722(24)	8.5402(4)
Fe1-Fe1[c]	9.0556(10)	8.8207(2)	8.9463(23)	8.8402(3)
Σ	66.96	44.25	65.35	45.35

[a] x, y, z+1; [b] x+1, y, z; [c] x, y+1, z

Table S3. Selected interatomic distances (Å), angles (°) and Σ (°) values for compounds **3** and **4**.

Compound	**3**		**4**	
Temperature	**250 K**	**80 K**	**250 K**	**90 K**
Spin state	**HS**	**LS**	**HS**	**HS**
Fe-N1(py)	2.2123(22)	2.0200(38)	2.2042(30)	2.2091(19)
Fe-N31(py)	2.2342(24)	2.0388(37)		
Fe-N14(tr^{py})	2.1712(23)	2.0056(41)	2.1539(28)	2.1512(18)
Fe-N44(tr^{py})	2.1480(23)	1.9836(37)		
Fe-N24(tz)	2.1941(25)	1.9855(38)	2.1582(30)	2.1485(18)
Fe-N54(tz)	2.1615(23)	1.9934(39)		
Fe-N(average)	2.1869(24)	2.0045(41)	2.1719(30)	2.1695(19)
N1(py)-Fe-N14(tr^{py})	75.53(9)	80.61(16)	76.94(11)	76.96(7)
N31(py)-Fe-N44(tr^{py})	75.85(9)	80.72(15)		
N1(py)-Fe-N24(tz)	85.52(9)	87.00(15)	92.18(11)	91.76(7)
N31(py)-Fe-N54(tz)	87.70(9)	88.45(15)		
N14(tr^{py})-Fe-N24(tz)	95.95(10)	91.45(16)	88.74(11)	88.71(7)
N44(tr^{py})-Fe-N54(tz)	98.04(9)	92.49(15)		
N1(py)-Fe-N31(py)	102.08(9)			
N1(py)-C2-C13-N14(tr^{py})	0.019(14)	-1.425(16)	11.639(5)	12.526(5)
N31(py)-C32-C43-N44(tr^{py})	1.990(14)	-0.991(16)		
Fe1-Fe1[a]	10.1083(14)	9.9547(16)	10.1925(3)	10.1812(3)
Fe1-Fe1[b]	14.7056(13)	14.3967(15)		
Fe1-Fe1[c]	9.9741(6)	9.8793(7)		
Fe1-Fe1[d]	8.5753(6)	8.2195(7)		
Σ	80.48	47.62	65.99	64.40

[a] x, y, z+1; [b] x+1, y, z; [c]; 1-x, -y, 1-z; [d] x, y+1, z

Table S4. Selected C-H···N and C-H···F interatomic contacts [Å] and angles [°] for **1** and **2** at 100 K and 240 K.

Compound									
	1					**2**			
Temperature	**100 K**		**480 K**		**Temperature**	**100 K**		**480 K**	
Spin state	**LS**		**HS**		**Spin state**	**LS**		**HS**	
D-H···A	d(D···A)	<DHA	d(D···A)	<DHA	*D-H···A*	d(D···A)	<DHA	d(D···A)	<DHA
C6-H6(py)···N13[a](tz[py])	3.153	140.23			*C5-H5(py)···F1[d]*			3.171	117.98
C6-H6(py)···N14[a](tz[py])	3.249	113.60			*C5-H5(py)···F22[d]*			3.442	157.58
C3-H3(py)···F2A	3.449	170.65	3.498	160.06	*C6-H6(py)···F1[d]*			3.136	118.68
C3-H3(py)···F2B			3.535	162.54	*C6-H6(py)···N13[a](tz[py])*	3.217	139.38		
C17-H17B(alkyl)···N12[b](tz[py])	3.379	132.20			*C16-H16A(alkyl)···F41*			3.410	151.87
C5-H5(py)···F4A[c]	3.255	127.26			*C16-H16A(alkyl)···F22*			3.053	164.25
C5-H5(py)···F4B[c]	3.224	126.70	3.302	135.77	*C16-H16A(alkyl)···F1*	3.433	146.84		
C5-H5(py)···F4C[c]			3.256	129.61	*C16-H16A(alkyl)···F3*	3.309	154.71		
C18-H18A(alkyl)···F3[d]	3.305	125.42			*C16-H16B(alkyl)···F4[b]*			2.866	111.83
C18-H18A(alkyl)···F1B	3.006	111.69			*C16-H16B(alkyl)···F31[b]*			3.482	152.55
C18-H18A(alkyl)···F4A[e]			3.507	171.37	*C16-H16B(alkyl)··· F41[b]*			3.102	110.80
C18-H18B(alkyl)···F4A[e]	3.368	170.36			*C17-H17A(alkyl)···F3[b]*	3.210	117.40		
C18-H18B(alkyl)···F2B[e]	3.561	160.17			*C17-H17B(alkyl)···F4[b]*			2.996	127.47
C16-H16A(alkyl)···F1A[d]	3.170	130.50	3.189	116.19	*C18-H18A(alkyl)···F1*	3.481	148.55		
C16-H16A···F1B	2.874	126.03			*C18-H18B(alkyl)···N13(tz[py])*	3.168	111.98	3.117	110.54
C16-H16A(alkyl)···F1B[d]			3.319	132.25	*C25-H25(tz)···F2[c]*	3.406	141.03	3.252	161.79
C16-H16A(alkyl)···F1C			3.150	128.21	*C25-H25(tz)···F21[c]*			3.167	143.38
C16-H16B(alkyl)···F2A	2.991	115.10			*C25-H25(tz)···F32[c]*			3.237	167.91
C16-H16B(alkyl)···N23(tz)	3.146	112.98	3.162	114.07					
C25-H25(tz)···F1A[f]	3.377	152.34	3.200	149.05					
C25-H25(tz)···F2C[f]			3.040	133.04					
C25-H25(tz)···F4B[f]	2.731	122.11							
[a] -x+1, -y, -z+2; [b] -x+2, -y, -z+1; [c] -x, -y+1, -z+1; [d] -x+1, -y+1, -z+1; [e] x+1, y, z; [f] -x+1, -y+1, -z					[a] -x, -y, -z+1; [b] -x+1, -y+1, -z; [c] x, y, z-1; [d] x-1, y, z+1				

Table S5. Selected C-H···N and C-H···F interatomic contacts [Å] and angles [°] for **3** at 80 and 250 K and for **4** at 90 and 250 K.

Compound									
	3					**4**			
Temperature	**80 K**		**250 K**			**Temperature**	**90 K**		**250 K**	
Spin state	**LS**		**HS**			**Spin state**	**HS**		**HS**	
D-H···A	d(D···A)	<DHA	d(D···A)	<DHA		*D-H···A*	d(D···A)	<DHA	d(D···A)	<DHA
C5-H5(py)···F11[a]	3.184	120.78	3.214	128.33		*C6-H6(py)···F3*[a]	3.055	112.6	3.131	114.18
C5-H5(py)···F14[a]	3.277	145.65	3.350	156.64		*C15-H15(tr)···F4*[b]	3.098	144.5	3.119	144.17
C6-H6(py)···N44[b]*(tz)*	3.120	114.42				*C16-H16A(alkyl)···F3*[c]	3.352	154.3	3.417	158.79
C15-H15(tr)···N53(tz)	3.131	115.28				*C16-H16B(alkyl)···F4*[b]	3.374	136.1	3.370	138.88
C16-H16A(alkyl)···F11[c]	3.130	111.09				*C18-H18A(alkyl)···F2*	3.128	143.3	3.184	143.49
C17-H17A(alkyl)···F231[d]	3.423	151.98	3.431	147.66		*C18-H18B(alkyl)···F4*[b]	3.404	145.5		
C18-H18B(alkyl)···F211	3.204	123.66	3.186	130.15		*C25-H25(tz)···F1*	3.128	153.8	3.139	154.54
C25-H25(tz)···F23[d]	3.149	136.13	3.184	137.71		*C99-H99B(MeOH)···N21*[c]*(tz)*	3.279	140.9		
C25-H25(tz)···F24[d]	3.346	137.91	3.389	145.47		*C99-H99B(MeOH)···N22*[c]*(tz)*	3.502	154.9		
C25-H25(tz)···F211[d]	3.309	166.47	3.479	164.84		*C99-H99A(MeOH)···N11(tr)*	3.650	170.8		
C25-H25(tz)···F231[d]	3.270	136.09	3.046	138.66		*C99-H99A(MeOH)···N12(tr)*	3.053	156.9	3.175	119.61
C35-H35(py)···N52[e]*(tz)*	3.159	126.41	3.252	128.13						
C35-H35(py)···F21[e]	3.232	129.11	3.281	138.48						
C35-H35(py)···F211[e]	3.369	136.39								
C45-H45(tr)···N23[f]*(tz)*	3.066	114.83	3.210	120.72						
C46-H46A(alkyl)···F21[g]	3.496	158.81	3.422	151.18						
C46-H46A(alkyl)···F22[g]	3.110	110.81								
C46-H46A(alkyl)···F221[g]	3.085	133.05	3.098	124.93						
C47-H47B(alkyl)···F23	3.268	129.12								
C47-H47B(alkyl)···F221	3.183	116.42	3.226	119.50						
C48-H48A(alkyl)···F13	3.145	158.07	3.238	159.50						
C48-H48B(alkyl)···F11[b]	3.238	120.86								
C55-H55(tr)···F14	3.167	161.86	3.266	167.84						
C98-H98A(MeCN)···N12[d]*(tr)*	3.540	150.97								
C98-H98A(MeCN)···F22	3.208	117.46	3.294	125.50						
C98-H98A(MeCN)···F231	3.189	116.58	3.316	130.14						
C98-H98C(MeCN)···F12	3.042	116.21	3.130	118.01						
[a] -x, -y, -z+1; [b] -x+1, -y, -z+1; [c] x, y+1, z; [d] -x, -y, -z; [e] x, y-1, z; [f] x+1, y, z+1; [g] -x+1, -y, -z						[a] -x+1/2, y+1/2, -z-1/2; [b] x, -y, z+1/2; [c] -x+1/2, -y-1/2, -z				

Table S6. Comparison between the calculated and experimentally determined Fe-N bond distances (in Å) for the central Fe1 in **1**-**4**.

Compound	**1**				**2**			
Spin state	HS		LS		HS		LS	
Fe-N / Å	Exp.	Calc.	Exp.	Calc.	Exp.	Calc.	Exp.	Calc.
Fe-N1(py)	2.186	2.152	2.013	2.018	2.188	2.202	2.036	2.043
Fe-N14(tz^{py})	2.138	2.126	1.968	1.980	2.131	2.136	1.971	1.969
Fe-N24(tz)	2.197	2.185	1.976	1.993	2.141	2.160	1.973	1.981
Fe-N(aver.)	2.174	2.154	1.986	1.997	2.153	2.166	1.199	1.998
Compound	**3**				**4**			
Spin state	HS		LS		HS		LS	
Fe-N / Å	Exp.	Calc.	Exp.	Calc.	Exp.	Calc.	Exp.	Calc.
Fe-N1(py)	2.212	2.166	2.020	2.028	2.204	2.232		2.014
Fe-N31(py)	2.234	2.231	2.039	2.037				
Fe-N14(tr^{py})	2.171	2.135	2.006	1.974	2.154	2.183		2.008
Fe-N44(tr^{py})	2.148	2.084	1.984	1.978				
Fe-N24(tz)	2.194	2.226	1.986	1.987	2.158	2.154		1.952
Fe-N54(tz)	2.162	2.191	1.993	1.981				
Fe-N(aver.)	2.187	2.172	2.005	1.998	2.172	2.190		1.991

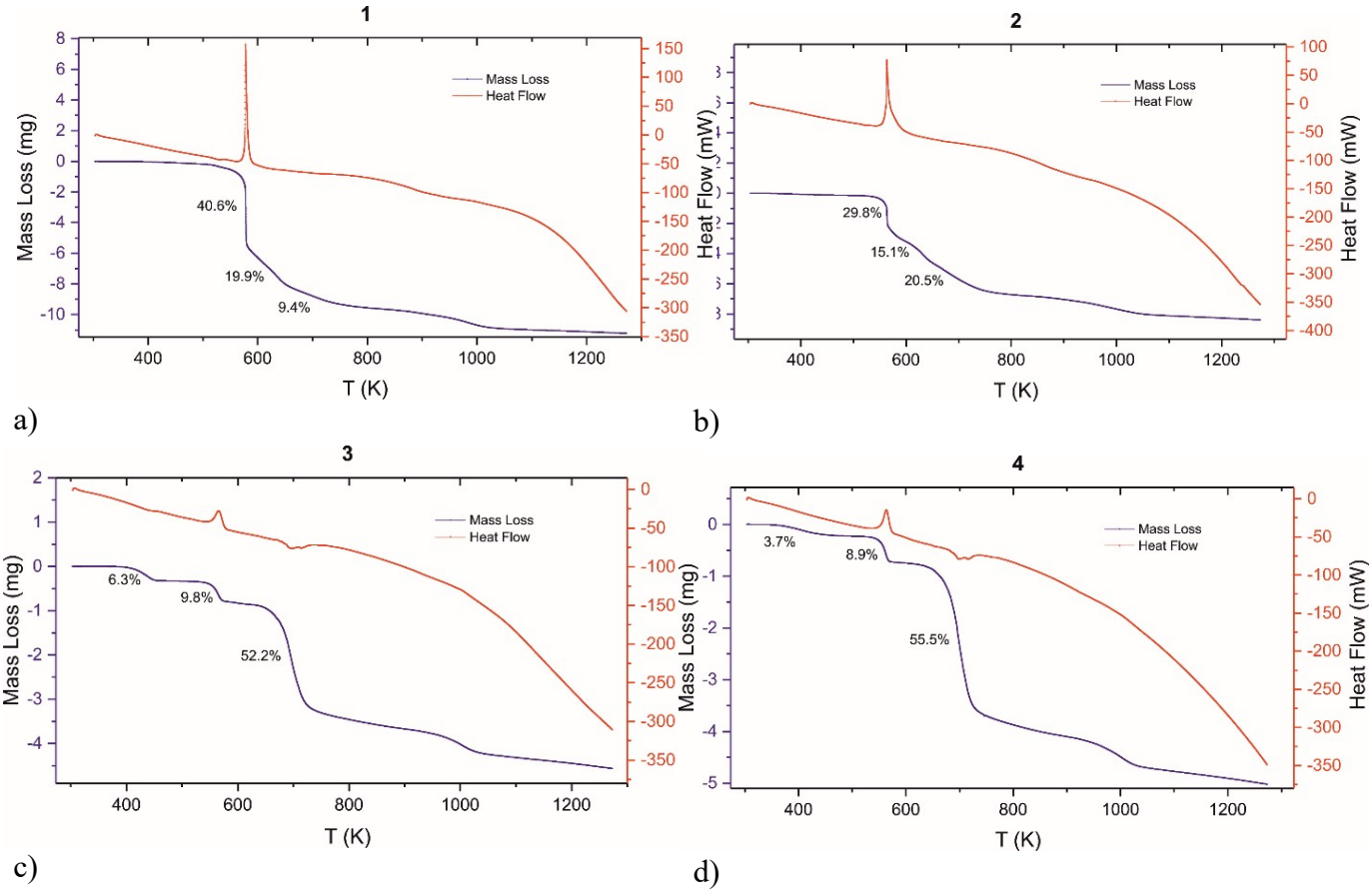

Figure S1. Results of thermogravimetry analysis for complexes **1** (a), **2** (b), **3** (c), **4** (d).

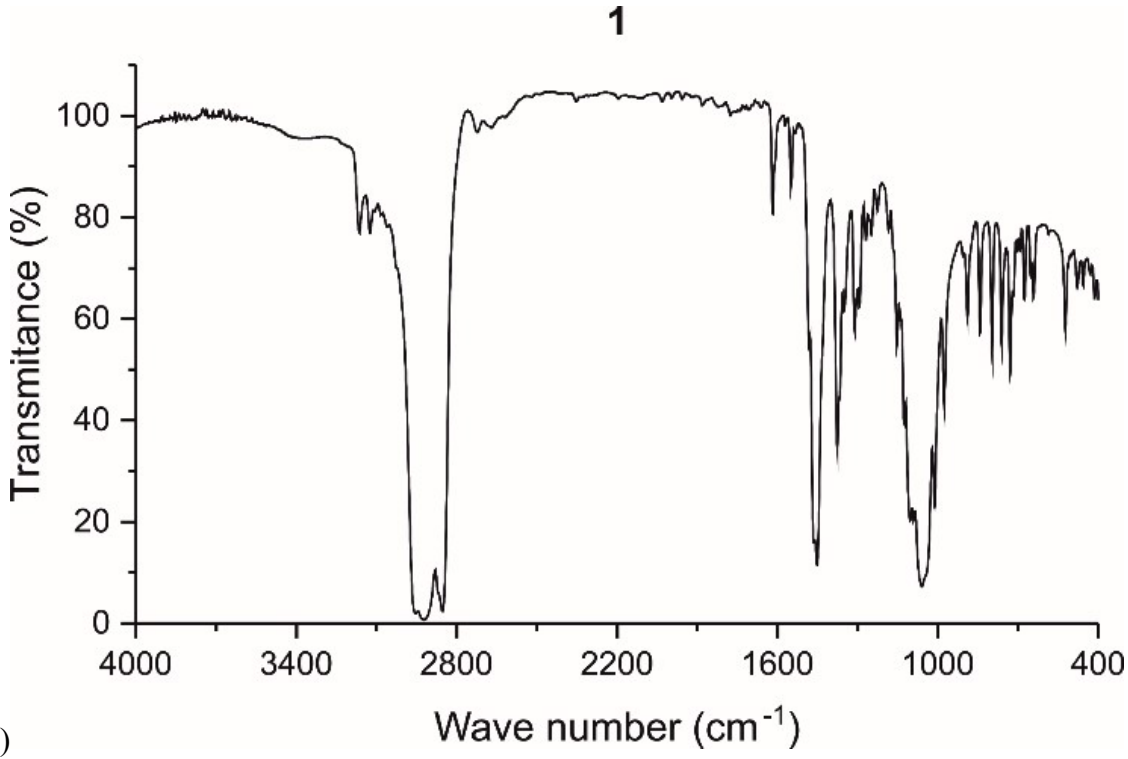
1
Transmitance (%)
100
80
60
40
20
0
4000
3400
2800
2200
1600
1000
400
Wave number (cm-1)

a)

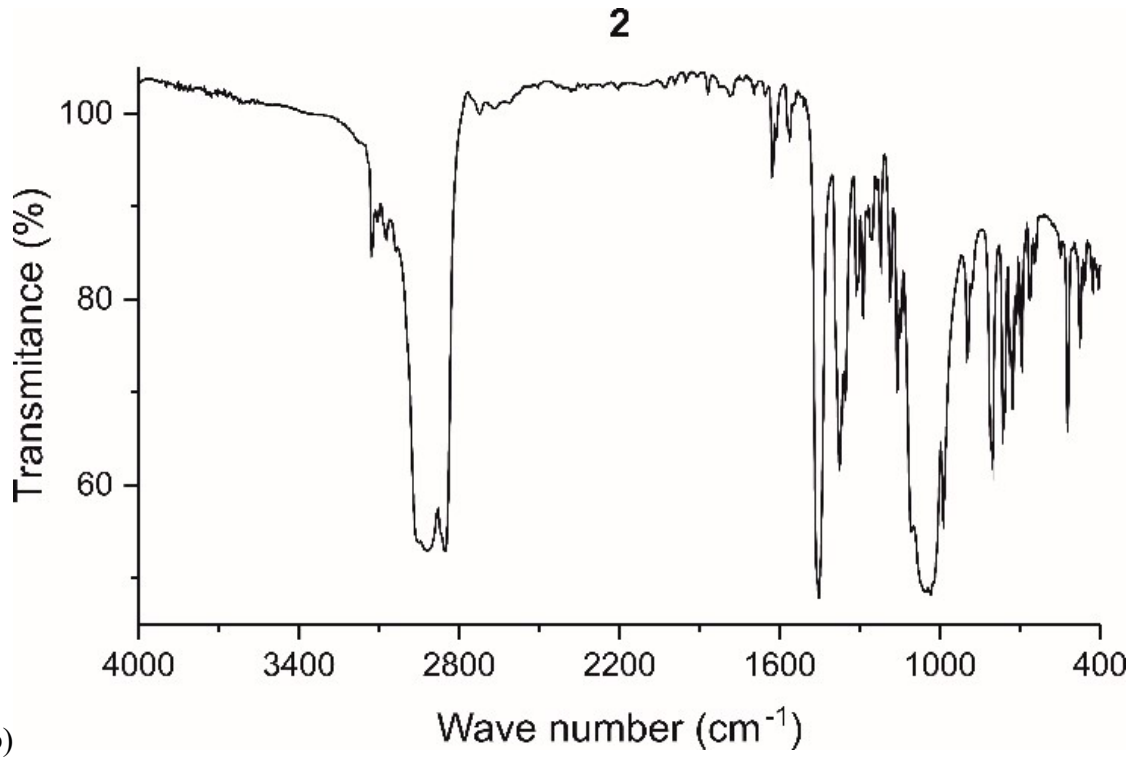
2
Transmitance (%)
100
80
60
4000
3400
2800
2200
1600
1000
400
Wave number (cm-1)

b)

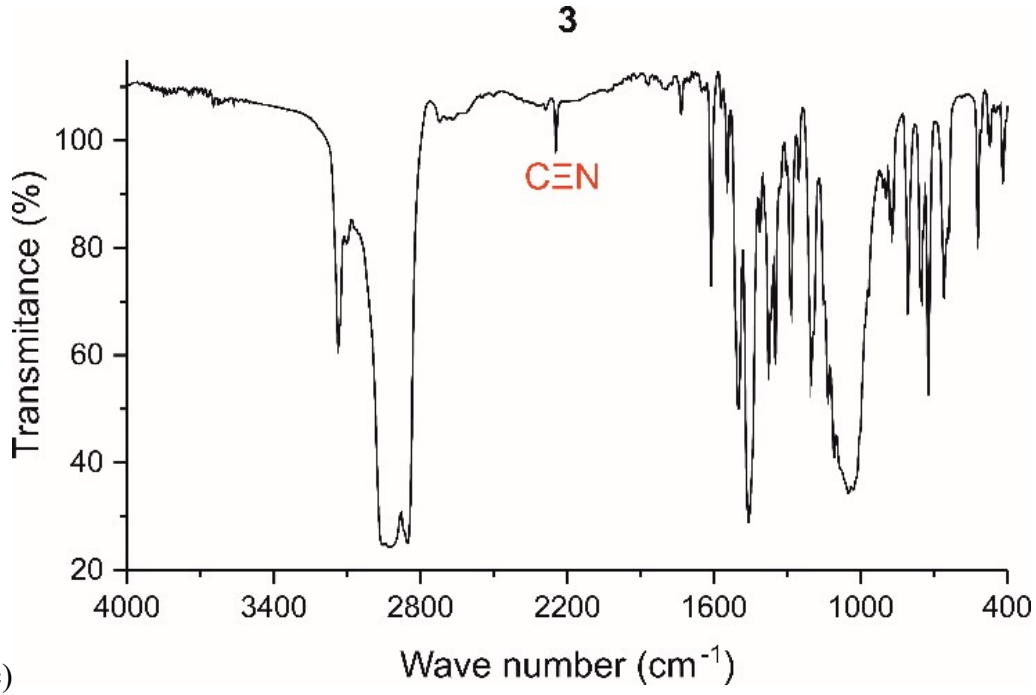

c)

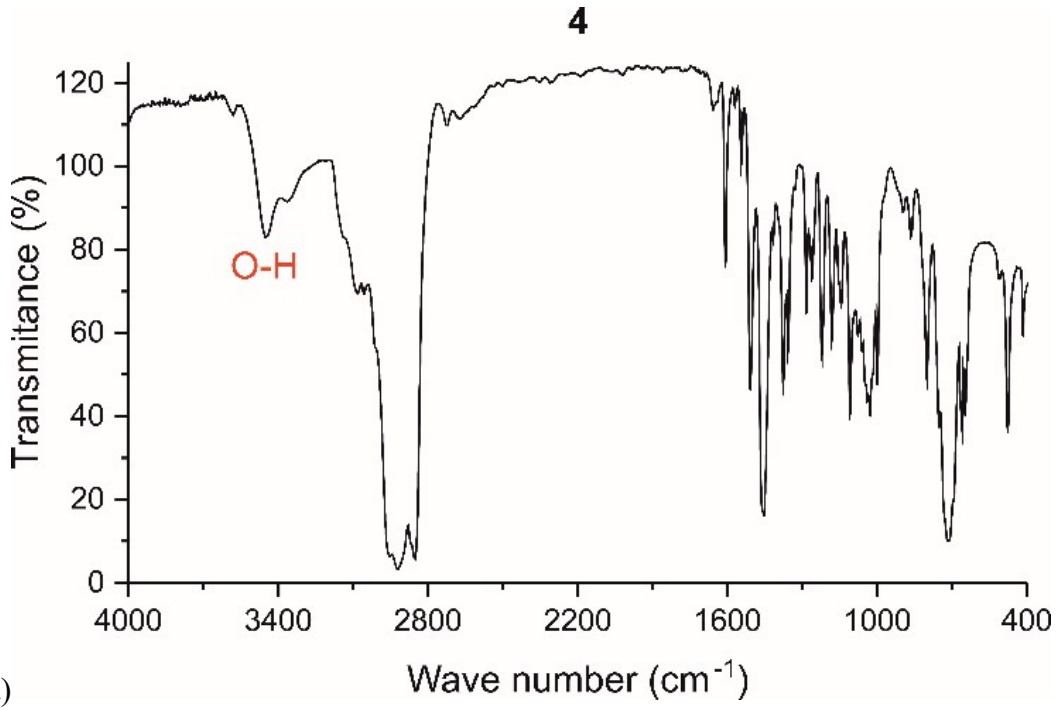

d)

Figure S2. FTIR spectra of **1** (a), **2** (b), **3** (c) and **4** (d) at RT (Nujol**).**

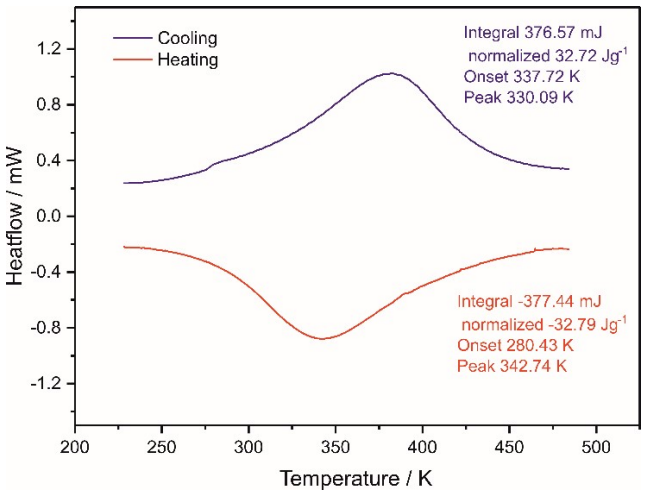

a)

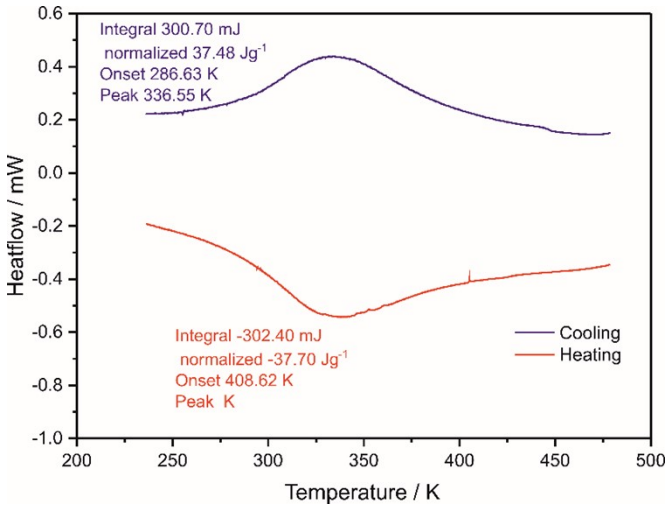

b)

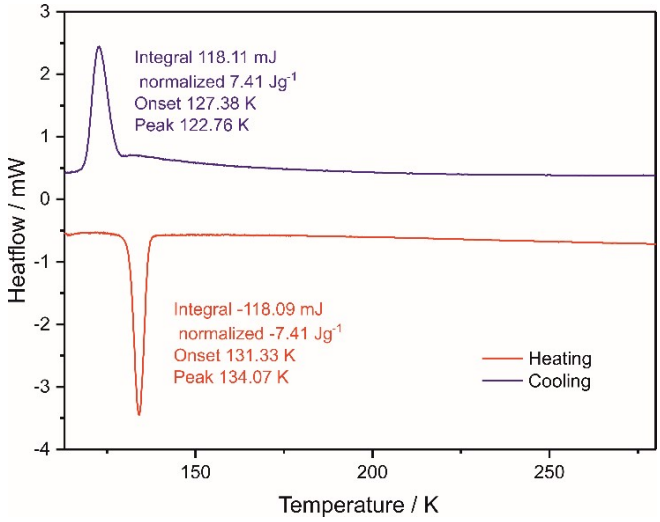

c)

Figure S3. Results of DSC studies for **1** (a)**, 2** (b) and **3** (c).

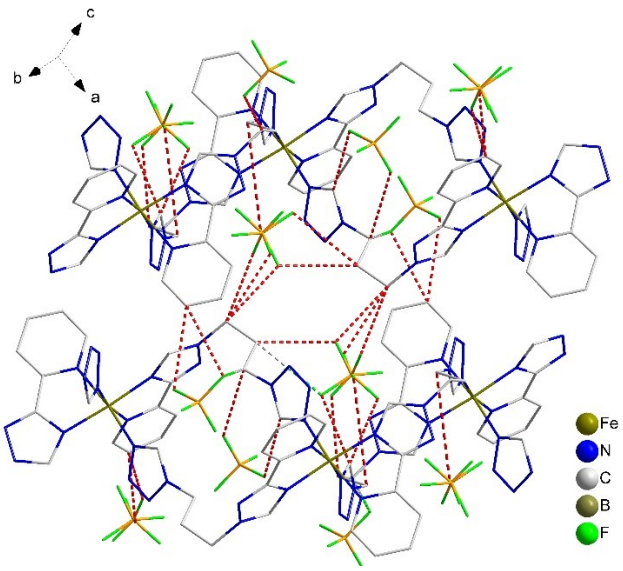

a)

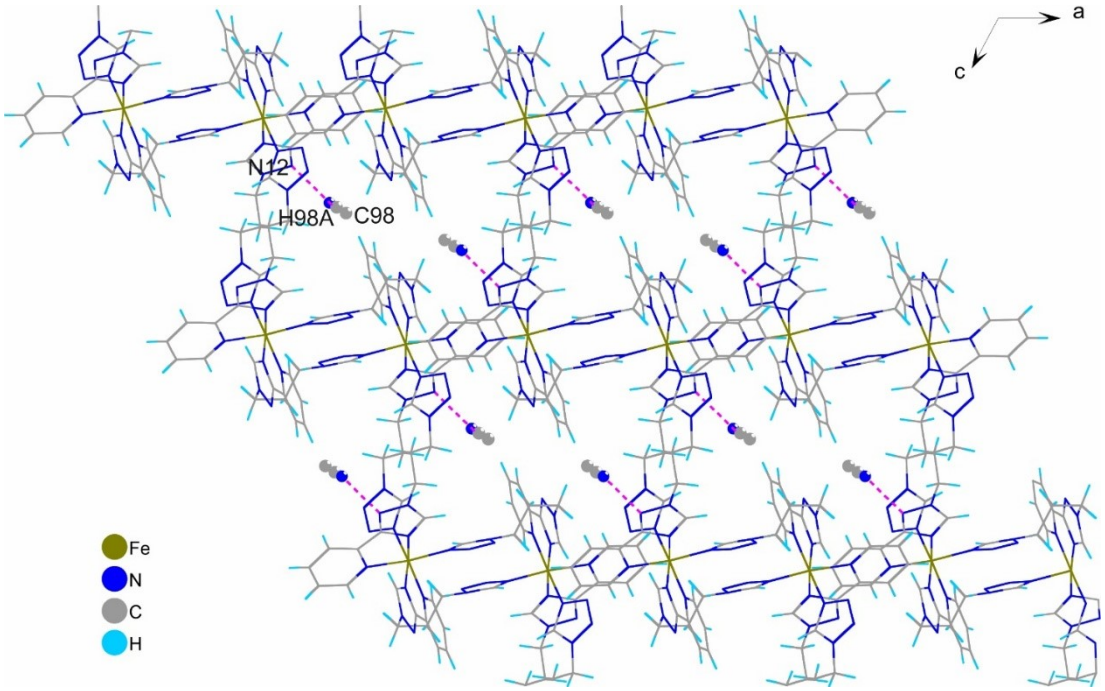

b)

Figure S4. Intermolecular contacts involving polymeric skeletons and anions (a) as well as noncoordinated acetonitrile molecules (b) in **3**.

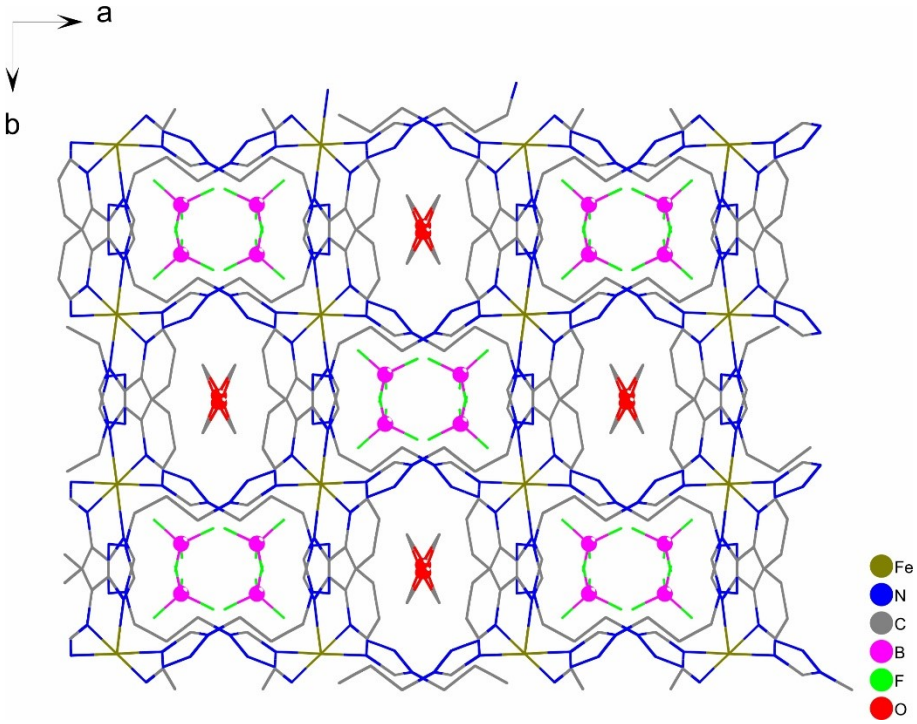

Figure S5. View along *c* direction showing perpendicular arrangement of chains forming adjusted layers in **4**.

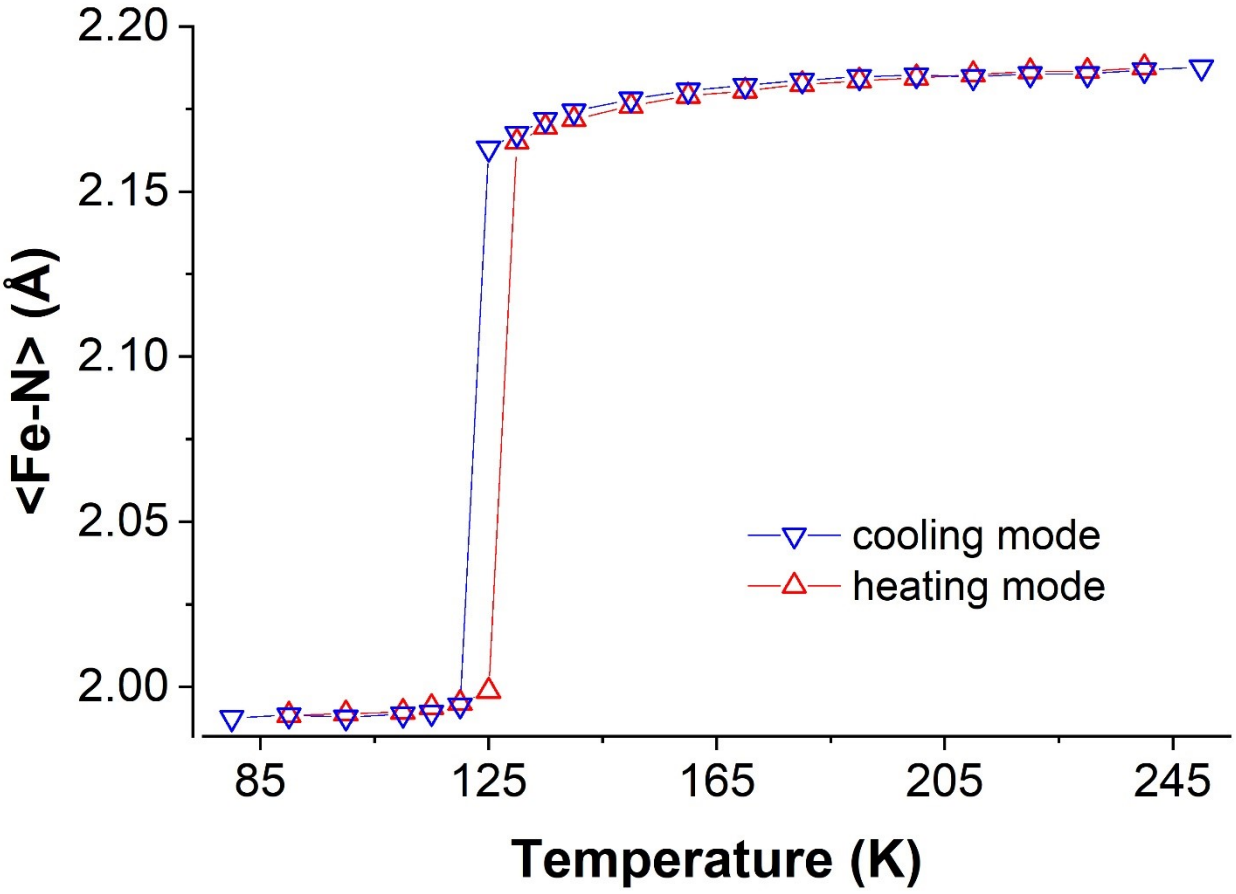

Figure S6. Temperature dependence of average <Fe-N> distances in **3**.

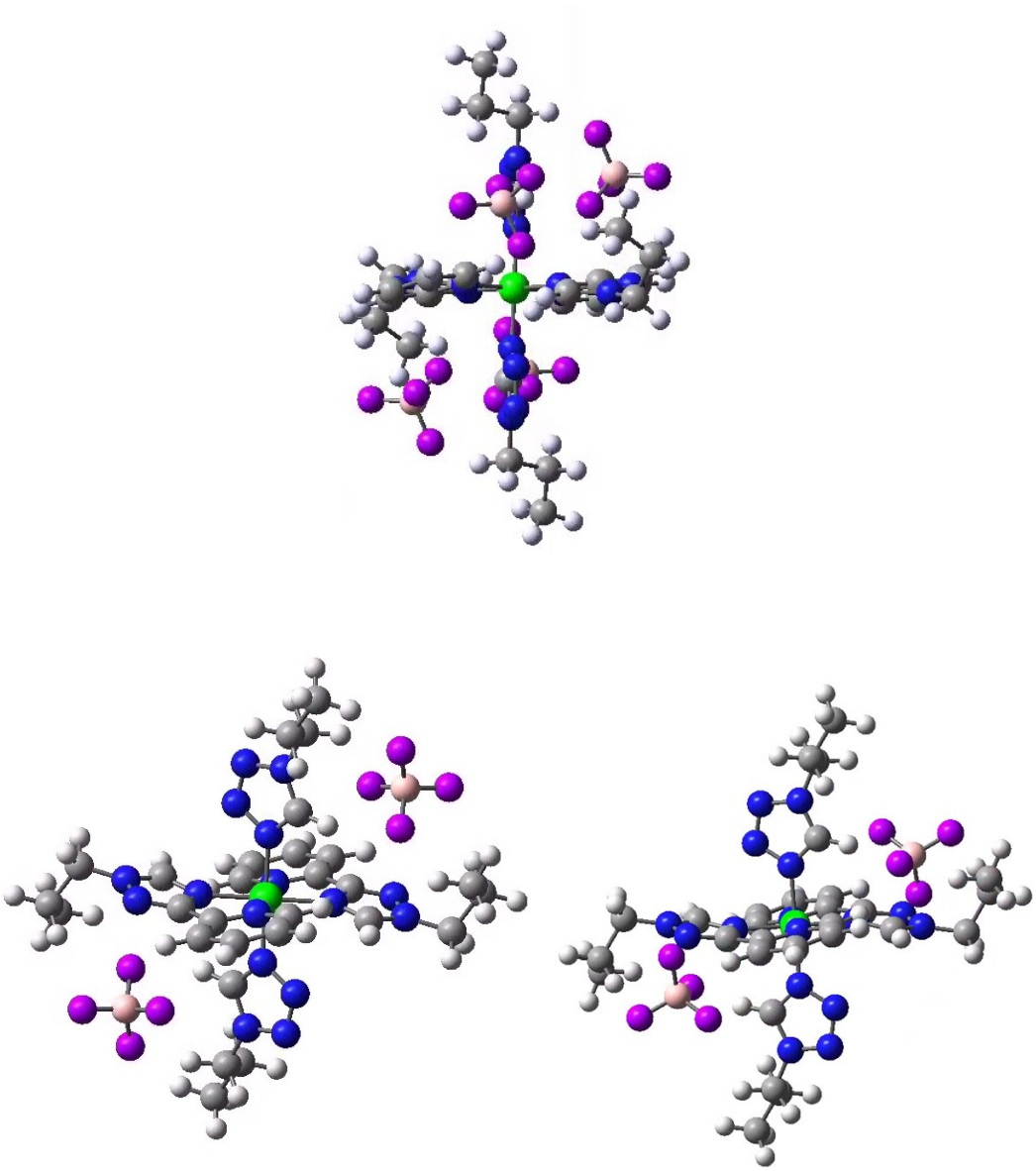

Figure S7. *Dist* (left) and *prox* (right) geometries of the FeN_6-dication – BF_4^- unit for the model of **4**. The orientation for the LS isomer is shown. The molecule of the complex with four anions around is shown on the top.

Thermodynamic effects of vibrations in low-spin and high-spin state. Here we consider the entropic and energetic effects of the vibrations, show the temperature dependence of estimated free enthalpy of the spin transition and analyse the contributions of modes of different energy regions to the vibrational entropy. The calculated temperature dependence of the vibrational entropy is shown in Figure 9. One clear conclusion is that within the complexes with *trans*-coordinated tetrazoles, it is the complex **1** for which the vibrational contribution to entropy at $T_{1/2}$ = 350 K is ca. 100 $J \cdot K^{-1} \cdot mol^{-1}$ higher than that for **2.** Thus, although the ligand

field reflected in the value of E_{el} for **1** is higher than that for **2,** there is an additional entropic stabilisation of the HS-state of **1.** The ΔS_{vib} for the HS-only complex **4** lies between those for **1** and **2** and is ca. 50 $J \cdot K^{-1} \cdot mol^{-1}$ higher at T = 100 K than that for the model of its *zig-zag cis*-coordinated polymorph **3**.

The contribution of the vibrational energy to the spin transition energy may be given quantitatively as zero-point correction (ZPE), i.e. the difference of the vibrational energy at 0 K, and the thermal contribution to energy (ΔE_{vib}) at 298.15 K.

If one considers only the metal-ligand vibrations the ΔE_{vib} corresponding to the LS → HS transition shall be negative as the vibrations for the LS isomer occur at higher energy than those of the HS isomer. On the other hand, with the increase of temperature these are the excited vibrational states of the HS isomer which are more effectively populated and the vibrational contribution becomes less negative. In consequence, the sum of the electronic and the vibrational contribution to the spin transition enthalpy increases with temperature. In our case the values of ZPE/ΔE_{vib} (ZPE = zero point energy or zero-point correction) are -52/-30, -56/-39, -44/-24 and -46/-24 $kJ \cdot mol^{-1}$ for the pentanuclear models **1**, **2**, **3** and **4**, respectively, making a significant contribution to the energy of spin transitions.

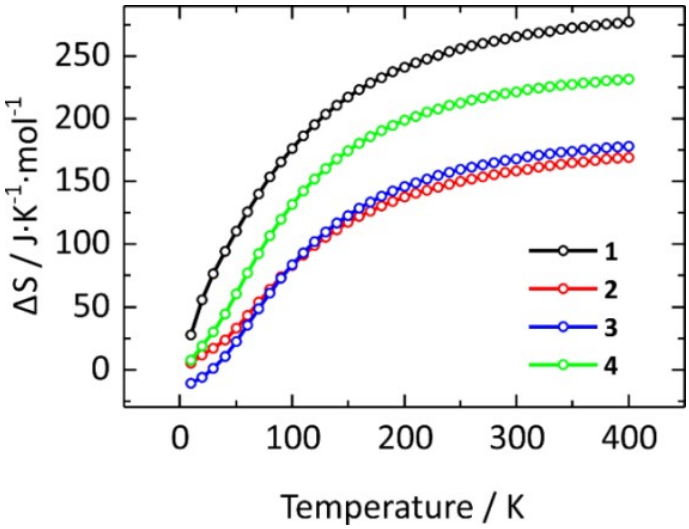

Figure S8. Calculated (B3LYP/CEP-31G, dispersion correction) vibrational entropies as a function of T for the pentanuclear models of the complexes under study. The solid line is a guide for the eye.

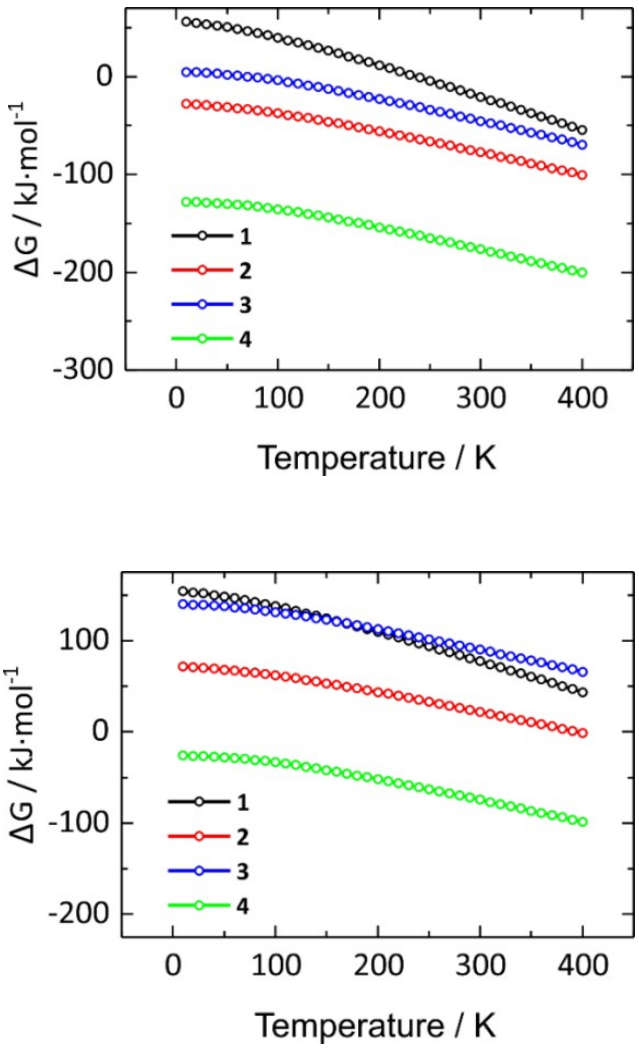

Figure S9. Calculated free enthalpy of the full (five Fe(II) centres) spin transition in pentanuclear models of the complexes under study. Top: the results for the structures optimised with B3LYP/CEP-31G and dispersion correction. Bottom: the results for the same geometries calculated with B3LYP*/CEP-31G (no dispersion correction). The solid line is a guide for the eye

The obtained temperature-dependent values of the vibrational entropy ΔS_{vib} and energy differences ΔE_{vib} were used to calculate the temperature dependencies of the free enthalpy of the spin-transition ΔG shown in Fig. S9. They illustrate the influence of the vibrational effects on the thermodynamics of the spin transition

It seems that entropic effects fairly compensate the difference in E_{el} between **1** and **2** and additionally stabilise the HS-state of **4**.